Biophysical Chemistry 154 (2011) 35–40

Contents lists available at ScienceDirect

Biophysical Chemistry

journal homepage: http://www.elsevier.com/locate/biophyschem

On stabilization of a neutral aromatic ligand by π–cation interactions in monoclonal antibodies

Chen Lin [a,1], Raja Chinnappan [a,1], Khem Acharya [a], Jean-Luc Pellequer [b], Ryszard Jankowiak [a,*]

[a] Department of Chemistry, Kansas State University, Manhattan, KS 66506, USA
[b] CEA, iBEB, Department of Biochemistry and Nuclear Toxicology, F-30207, Bagnols sur Cèze, France

ARTICLE INFO

Article history:
Received 4 November 2010
Received in revised form 13 December 2010
Accepted 14 December 2010
Available online 22 December 2010

Keywords:
Monoclonal antibody
Fluorescence
Pyrene
Laser-based spectroscopy

ABSTRACT

It has been shown that *anti*-PAH mAb can bind a particular cross-reactant by adopting two distinct "red" and "blue" conformations of its binding sites [N.M. Grubor et al. PNAS 102, 2005, 7453–7458]. In the case of red conformation of pyrene (Py)/*anti*-PAH mAb (with a broad fluorescence (0,0)-band with fwhm ~140 cm^{-1}), the central role in complex formation was played by π–π interactions. The nature of the blue-shifted conformation with very narrow fluorescence (0,0)-band (fwhm ~75 cm^{-1}) was left unclear due to the lack of suitable data for comparison. In this work, we suggest spectroscopic and modeling results obtained for the blue conformation of Py in several mAb (including 4D5 mAb) are consistent with π–cation interactions, underscoring the importance of π–cation interaction in ligand binding and stabilization in agreement with earlier modeling studies [J-L. Pellequer, et al. J. Mol. Biol. 302, 2000, 691–699]. We propose considerable narrowing of the fluorescence origin band of ligand in the protein environment could be regarded as a simple indicator of π–cation interactions. Since 4D5 mAb forms only the blue-shifted conformation, while *anti*-PAH and 8E11 mAbs form both blue- and red-shifted conformations, we suggest mAb interactions, with Py molecules lacking H-bonding functionality, may induce distinct conformations of mAb binding sites that allow binding by π–π and/or π–cation interactions.

1. Introduction

Antibodies (Ab) possess exceptional capability to selectively recognize and reversibly bind target molecules against which they are raised, as they exhibit a marked ability to acquire new functions [1]. Binding strength and binding selectivity in Ab-ligand interactions are mainly the consequence of salt bridges, hydrogen bonds, and van der Waals contacts [2]. It is believed antigen-binding promiscuity of a monoclonal antibody (mAb) is largely due to structural flexibility and conformational multiplicity of its binding sites. There are many examples in the literature of non-specific (cross-reactive) Ab [3,4] with their cross-reactivity ranging from broad promiscuity (where mAb binds molecules that are not structurally related), sometimes even with several orders of magnitude in size difference [5] to so-called group specificity (where an antibody recognizes a family of molecules with similar structural features but ignores structurally unrelated molecules) [6–8]. Unfortunately, the relationship between mAb structure and function, including the mode of interaction, is often unknown and therefore studies in this area continue to be of interest in biochemical and bioanalytical sciences.

One particularly large group of biologically important molecules of interest is polycyclic aromatic hydrocarbons (PAH), their metabolites, and PAH-derived DNA-adducts. Among them, special attention has been paid to benzo[a]pyrene (BP) and its derivatives due to their ubiquitous potency toward cellular DNA damage and the subsequent carcinogenicity of these processes [9 and references therein]. Depending on the metabolic activation pathway, BP-derived DNA adducts may possess a pyrene (Py) moiety that could reveal different modes of interaction with various mAb binding pockets. For example, our recent work has established the applicability of cross-reactive mAbs for highly specific analyses of complex stereoisomeric mixtures using fluorescence line-narrowing spectroscopy (FLNS) [10,11]. The highly promiscuous *anti*-PAH mAb can be used for capturing and analysis (detection, differentiation, and structural analysis) of not only structurally related PAHs (i.e., fluoranthene, Py, BP) but also their metabolic derivatives (i.e., diastereomeric BP-tetrols, BPTs) [11]. We have also shown that FLNS can identify various ligands cross-reacted with mAb [11], and that mAb can bind a particular cross-reactant by adopting two distinct conformations of its binding sites. We argued that, in the case of the "red-shifted" conformation of Py/*anti*-PAH mAb (with a broad (0,0)-band at 373.7 nm; full width at half maximum (fwhm) of ~140 cm^{-1}), the central role in complex formation was played by π–π interactions [10]. However, the nature of the "blue-

Abbreviations: Ab, antibody; Arg, arginine; mAb, monoclonal antibody; BP, benzo[a]pyrene; BPDE, benzo[a]pyrene diolepoxide; BPT, benzo[a]pyrene tetrol; CE, capillary electrophoresis; FLNS, fluorescence line-narrowing spectroscopy; fwhm, full width at half maximum; LIF, laser-induced fluorescence; Lys, lysine; NLN, non line-narrowed; PAH, polycyclic aromatic hydrocarbon; PBS, phospate-buffered saline buffer; Py, pyrene; ZPL, zero-phonon lines; Γ_{inh}, inhomogeneous broadening.

* Corresponding author. Tel.: +1 785 532 6785; fax: +1 785 532 6666.
E-mail address: ryszard@ksu.edu (R. Jankowiak).

[1] Both authors equally contributed to this work.

0301-4622/$ – see front matter © 2010 Elsevier B.V. All rights reserved.
doi:10.1016/j.bpc.2010.12.005

shifted" conformation of Py/*anti*-PAH mAb with the narrow fluorescence (0,0)-band at 372.3 nm (fwhm ~75 cm^{-1}) was not discussed in detail due to lack of suitable data for comparison.

In this work, we investigate the nature of the blue-shifted conformation of the Py/*anti*-PAH mAb complex by comparison with the conformation of pyrene in 4D5 and 8E11 mAb complexes. The 4D5 mAb has been selected as previous modeling studies [12] revealed π–cation interactions as an important factor in ligand binding; in fact, it has been suggested that proteins may use neutral, aromatic side chains to stabilize bound cationic ligands through π–cation interactions [13]. Though not confirmed experimentally for PAHs, it is well known that cation-π interactions are among the strongest of noncovalent forces [14]. For example, these interactions are important in horseradish peroxidase, where it was shown that an active site arginine (Arg) was essential to aromatic donor binding [15].

We explore the importance of π–cation and amino-aromatic interactions in biological molecular recognition using low-temperature, laser-induced fluorescence spectroscopy in both low- and high-resolution (FLNS) modes [9,16–18] and modeling studies. We confirm the presence of π–π interaction in the previously studied *anti*-PAH mAb [10,11] and suggest that a neutral aromatic ligand can also be stabilized by the π–cation interactions in the protein aromatic ligand/mAb complex. We argue the latter mode of interaction leads to very small inhomogeneous broadening (Γ_{inh}) and different energy of the origin-band than that expected for π–π interactions. We propose differences observed in Γ_{inh} and position of the (0,0)-bands could be used to provide information on the binding mode between various ligands and mAb.

2. Materials and methods

2.1. Low-temperature fluorescence spectroscopy

For laser-induced fluorescence (LIF)-based spectroscopic measurements (under non-line-narrowing (NLN) conditions), laser excitation at 308 nm was provided by a Lambda Physik Lextra 100 XeCl excimer laser. For FLNS measurements, the same laser was used as a pump source for a Lambda Physik FL 2002 Scanmate tunable dye laser system (10 Hz). A 1-m McPherson monochromator (model 2601) and a Princeton Instruments photodiode array were used for dispersion and detection of fluorescence. A Princeton Instruments FG-100 pulse generator was used for time-resolved spectroscopy with detector delay times from 0 ns to 160 ns and a gate width of 200 ns. For all spectroscopic measurements, 30 μL volumes of free pyrene (Py) and/or Py/mAb complexes were placed in quartz tubes and immersed in a helium cryostat with quartz optical windows. To ensure quantitative binding of ligands, immunocomplexes were formed by incubation of a 10-fold excess of mAb relative to the concentration of ligands ($2–5\times10^{-7}$ M) in the phospate-buffered saline (PBS) buffer. All fluorescence spectra are the average of 10 one-second acquisitions unless stated differently. The resolution for FLN and NLN spectra was ± 0.05 nm and 0.2 nm, respectively. Thus, corresponding accuracy in vibrational frequencies for FLNS measurements is about ± 3 cm^{-1}.

2.2. Monoclonal antibodies (mAbs)

The purified *anti*-PAH mAb was purchased from Strategic Biosolutions, Newark, DE, USA. The 4D5 and 8E11 mAbs were obtained from Prof. Regina M. Santella (Columbia University, New York); the 4D5 hybridoma line was raised against a PAH-protein conjugate [19]; and the 8E11 mAb was raised against a BP-DNA conjugate [20]. The IgG type 8E11 and 4D5 mAbs were further purified in our laboratory from immobilized protein G resin (obtained from Pierce Inc. Rockford, IL). All buffers and the protein G resin were equilibrated to room temperature before use. (Protein G has strong binding affinity with IgG type mAbs). The immobilized protein G resin was packed in a 2-mL polypropylene column. The column was equilibrated by adding 5 mL of PBS buffer; the buffer was drained through the column. The sample was added to the column and allowed to flow completely into the resin (total content of the antibody was less than 80% of column capacity). Non-IgG components, if present, were washed from the resin using 15 mL of the PBS buffer. The bound IgG mAb was eluted by 5-mL of elution buffer (pH = 2–3; Pierce Inc.). The 0.5 mL fractions were collected and immediately neutralized using a 1-M Tris buffer (pH = 8.0). The IgG mAb-containing solution was dialyzed using a Slide-A-Lyzer Dialysis cassette (Pierce Inc.) against the PBS buffer. The final concentration of the mAb was measured from the UV absorption at 280 nm using a Nanodrop spectrophotometer, and mAbs were stored at −80 °C before use. Methanol and glycerol (Aldrich, Milwaukee, WI) were used as received. PBS buffer (0.1 M sodium phosphate and 0.15 M sodium chloride) was purchased from Pierce and prepared according to the procedure supplied by the manufacturer.

2.3. Ligands

The selection of Py for these studies was intentional for several reasons: *i)* its fluorescence spectra are sensitive to small changes in their microenvironment [21–23]; *ii)* spectral properties of Py under high-resolution fluorescence conditions are well understood and described [9–11,17,18,24]; and *iii)* Py and related molecules are among the most important environmental contaminants. BPDE-dG diastereomers ((−)-*trans*-BPDE-dG, (+)-*cis*-BPDE-dG, (−)-*cis*-BPDE-dG, and (+)-*trans*-BPDE-dG) were prepared by treating calf thymus DNA with (±)-*anti*-BPDE as described in ref. [25].

2.4. Computational methodologies

2.4.1. Docking of Py in mAb

The molecular model of the 4D5 mAb variable region was based on the structural template of antibody 17/9 (Protein Data Bank (PDB) code 1HIL) as described in ref. [12]. As before, the third complementarity determining region (CDR) of the light chain (L3) was built using the corresponding region in antibody HyHEL5 (PDB code 3HFL), whereas the short third CDR of the heavy chain (H3) was built by computer graphics. The final model was energy-minimized in X-PLOR using the CHARM22 force field as described previously [12]. Py has been docked into the binding pocket of 4D5 using AUTODOCK. The computation was set using a $64\times64\times64$ cubic grid with a spacing of 0.5 Å centered on the N atom of LysL89. Docking was performed using the simulated annealing procedure of AUTODOCK as described previously [26].

2.4.2. Transitions

The stabilization of Py by a cationic, protein side chain in the 4D5 mAb binding pocket was further studied by quantum mechanical calculations. Energies of the (0,0)-transitions of Py in the nine lowest-energy conformations of Py in 4D5 mAb were calculated using the HyperChem ZINDO/S method with configurational interaction. The overlap weighting factor for σ–σ and π–π were 1.267 and 0.585, respectively. (0,0)-transitions were also calculated for Py in water and mutated 4D5 mAb, where the cationic side chain Arg was replaced by glutamine (Glu). For Py in water the AMBER program was used to optimize geometry of Py and water molecules; a periodic box of $18.7\times18.7\times18.7$ $Å^3$ was used with the electrostatic and van der Waals scale factors of 0.833 and 0.5, respectively.

3. Results

3.1. Conformation of Py/4D5 mAb complex

It has been confirmed the binding site of the 4D5 mAb has an exceptionally deep antigen-binding pocket with two positively charged residues, LysL89 and ArgH95 (the latter nomenclature is

from ref. [12], where L and H stand for the light and heavy chains, respectively), which create substantial positive electrostatic potential in the binding pocket. Presence of LysL89 and ArgH95 in the binding pocket seems unusual given the hydrophobic nature of the PAHs; yet, these side-chain conformations could be reliably predicted. The role of these side chains has been studied before using side-directed mutagenesis *in silico* [12]. In the study of mutated 4D5 in the same paper, LysL89 was replaced by methionine, a neutral, linear side chain; and ArgH95 was replaced by glutamine, a polar but uncharged side chain. Neither the ArgH95Gln mutant nor the LysL89Met/ArgH95Gln double mutant showed detectable binding of benzo[*a*]pyrene to 4D5 using indirect enzyme-linked immunosorbent assays [12]. This was consistent with a surprisingly highly polar binding pocket, considering the hydrophobicity of the ligand. The π–cation interaction of Py with ArgH95 in 4D5 mAb is illustrated in Fig. 1, which shows the guanidino group of Arg has parallel position in respect to the Py plane. The distance between the Py plane and the guanidino group is around 3–4 Å. Thus, the Arg side chain that flanks one side of the binding pocket is essential for Py binding, suggesting a π–cation interaction stabilizes the bound PAH. It should be emphasized that no aromatic side chain is located in the deep binding pocket of 4D5 mAb. Lowest energy conformations of Py in the protein environment were further investigated by modeling studies to reveal whether the relative (calculated) shift of the (0,0) transition of Py inside the binding pocket is consistent with the experimental data.

3.2. NLN fluorescence spectra of Py complexed with anti-PAH and 4D5 mAbs

In Fig. 2, we compare binding of Py to *anti*-PAH and 4D5 mAb. The *anti*-PAH mAb is known to involve π–π [10,11], while 4D5 mAb (*vide supra*) should involve the π–cation interactions in ligand binding. The 4.2 K NLN fluorescence origin bands obtained for both Py/*anti*-PAH mAb and Py/4D5 mAb complexes are shown in frames A and B of Fig. 2, respectively. These NLN spectra were obtained with an excitation wavelength (λ_{ex}) of 308 nm in a PBS buffer (PBS) (spectra a, c) and glycerol/PBS (G/PBS; 1/1) buffer mixture (spectra b, d). The position of Py fluorescence emission maxima in PBS buffer (371.6 nm) and G/PBS (371.1 nm) glass are shown by the dashed and dotted vertical lines, respectively. Significant spectral differences are clearly observed with the 4D5 mAb, showing only one, i.e. the "blue"-shifted conformation (labeled as conformation I). NLN spectra for Py/8E11 revealed two conformations, i.e. conformation I (major) and conformation II (minor); spectra not shown for simplicity. (See FLN spectra d and e in Fig. 3 for further proof that conformation I is the major conformation in 8E11 mAb).

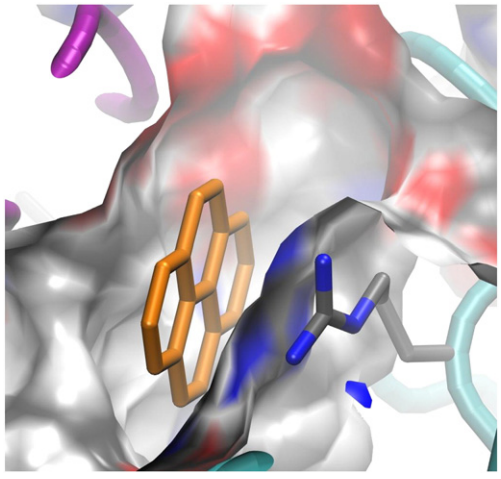

Fig. 1. Model of the 4D5 mAb fragment with Py (orange sticks) docked in the lowest binding energy conformation in the mAb binding pocket represented by its molecular surface. The tube in cyan is the heavy chain; tube in magenta corresponds to light chain. Only the ArgH95 and Py are displayed for clarity. The molecular surface is colored by atom type. Graphics was made using VMD [32].

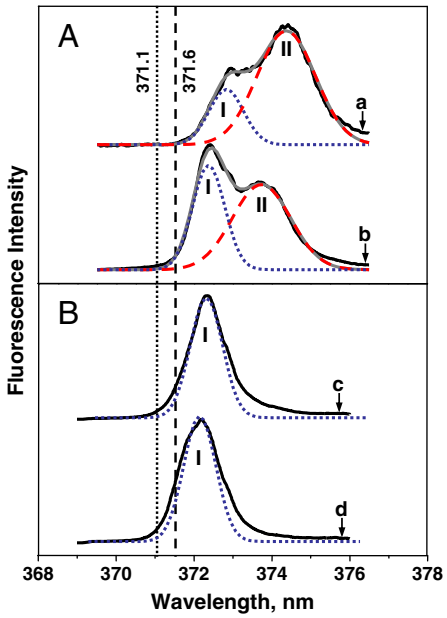

Fig. 2. Low temperature NLN fluorescence spectra of immunocomplexed Py in *anti*-PAH mAb (frame A) and 4D5 mAb (frame B). Spectra a,c and b,d were obtained in PBS and G/PBS (1/1) matrices, respectively. The dotted and dashed vertical lines indicate the position of the (0,0)-band of free Py in G/PBS (371.1 nm) and PBS (371.6 nm) matrices. To guide an eye, the bands assigned to conformations I and II are indicated by the dotted and dashed Gaussians respectively. $T = 4.2$ K; gate width, 200 ns; delay time, 40 ns; $\lambda_{ex} = 308$ nm.

As in the case of the Py/*anti*-PAH mAb complex studied previously [10], one of the conformations observed in this work (as shown in frame 2A) also possesses a significantly narrower fluorescence origin band (band I). To guide an eye, and for simplicity, the bands assigned to conformations I and II are indicated by dotted and dashed Gaussians, respectively. The fwhm of conformations I ("blue" conformation) and II ("red" conformation) are 75 cm^{-1} and 125 cm^{-1}, respectively. Spectral parameters for Py/mAbs complexes in different matrices are summarized in Table 1. Results shown in frame 2A (spectrum b) are in agreement with Ref. [10] and confirm the existence of two populations of Py in *anti*-PAH mAb that are trapped at low temperature. However, in this case, the G/PBS glass reveals relatively larger contribution from conformation I. The most striking difference between Py/*anti*-PAH mAb (frame 2A) and Py/4D5 mAb (frame 2B) is that the Py/4D5 mAb complex shows only conformation I. Its fwhm is similar to conformation I of Py/*anti*-PAH mAb, i.e. 75 ± 5 cm^{-1}, with a weakly matrix-dependent, blue-shifted origin band. The very narrow fluorescence origin band of conformation I (and smaller red-shift) in comparison with conformation II suggests that different modes of interaction between the Py moiety and the mAb binding pocket are present.

We have also found that the relative intensity ratio of band I to band II in *anti*-PAH mAb is matrix-dependent, as was clearly visible by comparison of spectra a and b in Fig. 2A. In the case of the Py/*anti*-PAH mAb complex, this ratio slightly depends on the relative amount of glycerol, i.e. the glass (matrix) composition, and on the cooling rate (data not shown). For example, fluorescence spectrum b shown in Fig. 2A has a relatively larger contribution from conformation I in comparison with data reported in Ref. [10], due to slightly different glass composition. This in turn suggests that the energy landscape can change due to conformational flexibility of protein. (Note, the heterogeneity of configurations in the binding pocket is responsible

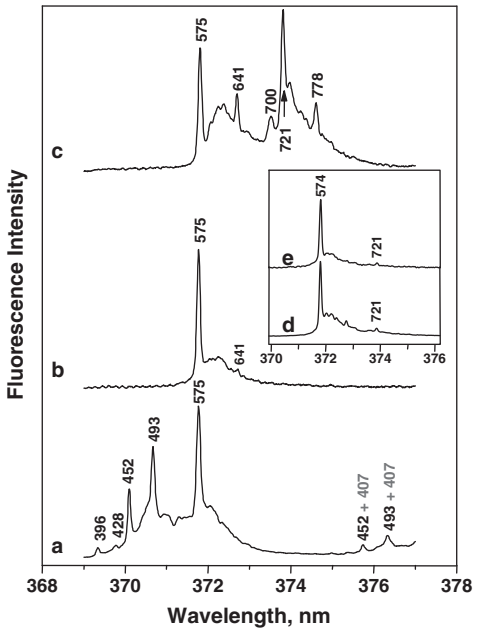

Fig. 3. FLN spectra of Py in various mAbs at $T = 4.2$ K obtained with λ_{ex} of 364 nm (vibronic excitation). Spectra a–c correspond to free Py, Py/4D5 mAb complex, and Py/anti-PAH complex in G/PBS (1/1) matrix, respectively. Spectra e and d in the inset show FLN spectra obtained for Py/8E11 mAb complex in PBS and G/PBS matrices, respectively; see text for details. The numbers above the peaks (i.e. the ZPL) correspond to the excited state vibrational frequencies in cm^{-1} (gate width = 200 ns, delay time = 40 ns). The 407 cm^{-1} mode corresponds to the ground state vibrational frequency of Py building on the zero-phonon lines at 452 and 493 cm^{-1}, respectively.

for the observed Γ_{inh}; the latter, however, has nothing to do with the presence of two different subpopulations of Py). The finding that only one conformation (i.e. blue-shifted conformation I) is observed in 4D5 mAb is consistent with the modeling studies that revealed a very deep and narrow binding pocket [12], suggesting less configurational diversity.

3.3. Calculated (0,0) bands

The experimentally observed shift of the (0,0)-band for conformation I of Py in 4D5 mAb, in comparison to solvated Py in both PBS buffer and PBS/Gly matrices, was about 1.3 nm. In contrast, our calculations showed the relative shift of the (0,0)-transition for the Py/4D5 mAb complex (for the nine calculated lowest-energy conformations), when compared with water-solvated Py, was about 4 nm. We anticipated the calculated red-shift of the (0,0) transition due to π–π interaction inside the binding pocket would lead to an even larger red-shift than observed experimentally; for example, calculated shift of the (0,0)-band for intercalated BPDE-DNA adducts (where π–π interaction plays a major role) are about 8–10 nm [unpublished results]. Unfortunately, mAb with a known structure and-well defined aromatic residues inside the binding pocket (to the best of our knowledge) is not available for calculations and direct comparison. Nevertheless, we suggest the trend observed in modeling studies is consistent with the experimental data. For example, the measured (0,0)-transition of the Py-like molecules (e.g. BPDE-DNA adducts) [17,27] intercalated between DNA bases undergoes a large (~3 nm) shift towards lower energies (due to π–π interaction) in agreement with the 2.5–3.0 nm red-shift observed in this work for conformation II (see Fig. 2), where π–π interaction plays a major role [10].

3.4. FLN spectra obtained for free Py and various Py/mAb complexes

Narrowness of the (0,0)-band of conformation I is clearly visible in the FLN spectra shown in Figs. 3–5, where the sharp peaks correspond to the resonant fluorescence zero-phonon lines (ZPL) emitting within the inhomogenously broadened absorption profile [16,17]. Since all spectra reported in this work were obtained using vibronic excitation, numbers above the sharp peaks in the main frames of Figs. 3–5 correspond to the excited state vibrational frequencies. The 4.2 K spectra a–c in Fig. 3 correspond to free Py, Py/4D5 mAb complex, and Py/*anti*-PAH mAb complex, respectively, and were obtained with λ_{ex} of 364 nm. Spectra e and d in the inset show FLN spectra of Py obtained for a different mAb (i.e. for Py/8E11 mAb complex) in PBS and glycerol/PBS matrices, respectively, and are nearly identical to spectrum b in the main frame of Fig. 3 obtained for the Py/4D5 mAb complex. This clearly indicates that Py in 8E11 mAb also adopts conformation I.

Spectra a, b, and c are distinctly different due to different band maxima; due to contribution from two conformations, the Py/*anti*-PAH mAb complex (spectrum c) shows vibrations over a broader energy range than spectrum b obtained for the Py/4D5 mAb complex. Spectra b, d, and e are consistent with a very narrow Γ_{inh} for conformation I as already indicated by the NLN spectra shown in Fig. 2. Although spectra e and d (for Py/8E11 MAb) are very similar to curve b (Fig. 3) obtained for the Py/4D5 mAb complex, the presence of the weak 721 cm^{-1} mode indicates (in agreement with the NLN spectra) that minor conformation II is also formed in 8E11 MAb. Note the FLN spectrum of Py (curve a of Fig. 3) also reveals several vibrational modes within its (0,0)-band due to a larger Γ_{inh} of about 160 cm^{-1}. Comparison of curves b and d in Fig. 2 with spectra c and b of Fig. 3 (for $\lambda_{ex} = 364$ nm) clearly indicates the 575 cm^{-1} mode observed in curve c corresponds to Py/*anti*-PAH mAb in conformation I. Higher frequency modes at 641 cm^{-1} (at least in part) and modes at 700, 721, and 778 cm^{-1} correspond to conformation II. Modes in this energy range correspond to the Py C–C–C and C–C–H out-of-plane vibrations [28].

Spectra shown in frames A and B of Fig. 4 were obtained with $\lambda_{ex} = 358.5$ nm and correspond to the FLN spectra of pyrene/4D5 mAb (curves a) and pyrene/*anti*-PAH mAb complexes (curves b) in PBS and G/PBS glasses, respectively. The dotted line above curve b in

Table 1
Spectral characteristics of Py/*anti*-PAH mAb and Py/4D5 mAb complexes in PBS and G/PBS (1:1) matrices at 4.2 K. Conformation I and II correspond to the "blue" and "red" conformations, respectively.

Matrix	Py/anti-PAH mAb complex				Py/4D5 mAb complex[a]				Py	
	Conformation I		Conformation II		Conformation I		Conformation II			
	(0,0)[b] ± 0.2 nm	fwhm[c] ± 5 cm^{-1}	(0,0) ± 0.2 nm	fwhm ± 5 cm^{-1}	(0,0) ± 0.2 nm	fwhm ± 5 cm^{-1}	(0,0) ± 0.2 nm	fwhm ± 5 cm^{-1}	(0,0) ± 0.2 nm	fwhm ± 5 cm^{-1}
PBS buffer	372.9	75	374.4	125	372.3	75	–	–	371.6	160
G/PBS matrix	372.4	75	373.6	125	372.1	75	–	–	371.1	160

[a] Py/8E11 mAb complex (non-line narrowed spectra not shown) showed also conformation I (major) and conformation II (minor) as discussed in text.
[b] Maximum of fluorescence (0,0)-band (in nm).
[c] fwhm is the full width at half maximum.

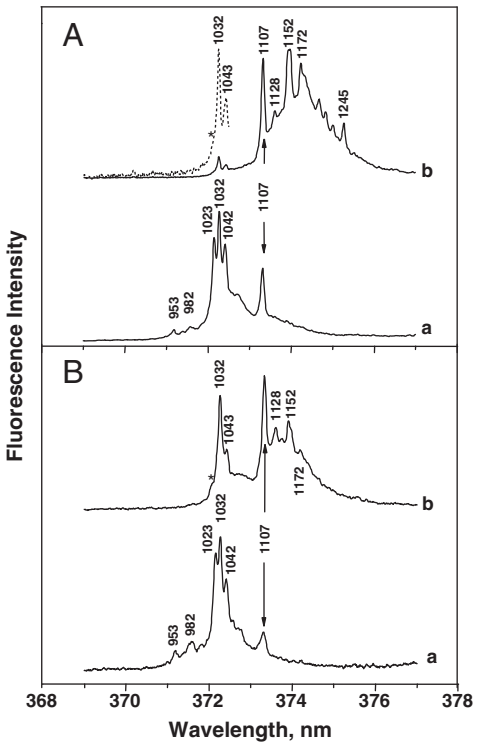

Fig. 4. Frame A: Spectra a and b show FLN spectra of Py/4D5 mAb and Py/*anti*-PAH complexes in PBS buffer, respectively, obtained with λex = 358.5 nm. The dotted line above curve (b) shows an expanded part of curve (a) to reveal the 1032 and 1043 cm^{-1} vibrational modes. Frame B: FLN spectra of Py/4D5 mAb (curve a) and Py/*anti*-PAH (curve b) complexes in G/PBS (1:1), respectively. $T = 4.2$ K, gate width = 200 ns, delay time = 40 ns. Asterisks label the position of 1023 cm^{-1} mode which is not resolved in FLN spectra of Py/*anti*-PAH mAb.

frame A shows an expanded part of curve b to show more clearly the 1032 and 1043 cm^{-1} vibrational modes. The latter two modes (1032 cm^{-1} and 1043 cm^{-1} in curve b, frame A) can be assigned to conformation I. Note these two modes, 1032 and 1042 cm^{-1}, are more intense in the G/PBS matrix (see curve b in frame B). The mode near 1023 cm^{-1} (indicated by a star in curves b of frames A and B, respectively) is not well resolved in Py/*anti*-PAH mAb independent of matrix composition. This mode, however, is well resolved for the Py/4D5 mAb complex in both PBS and G/PBS matrices (see curves a of Frames A and B in Fig. 4). Comparison of mode frequencies for conformation I (e.g. modes at 950–1107 cm^{-1}) in spectra for two different mAbs (see Fig. 4) reveals the binding pocket (due to slightly different interactions) can also influence the relative intensities of the vibrational frequencies, i.e. the relative mode intensity of conformation I varies depending on mAb. Note the Py modes in the range of 1020–1180 cm^{-1} correspond to C–C stretching modes and C–C–H in-plane bending modes [28]. Fig. 5 shows FLN spectra ($T = 4.2$ K, $\lambda_{ex} = 354$ nm) of free Py (curve a), immunocomplexed Py/4D5 mAb (curve b), and Py/*anti*-PAH mAb (curve c) in G/PBS glass. These spectra, along with data shown in Fig. 3, are consistent with our conclusion that Py adopts two conformations in *anti*-PAH mAb. Selective excitation of 354 nm (see curve c) reveals the minor contribution from conformation II (see modes at 1467–1558 cm^{-1}). However, independent of excitation, Py in 4D5 mAb shows only the blue-shifted conformation I. As discussed above, these two conformations are associated with a different mode of binding. Finally, note a different distribution of several vibrational modes in curve c of Fig. 5 labeled by stars. As mentioned above, such changes in the intensity of various vibrational modes are most likely due to differences in the composition and shape of the binding pocket. For example, a smaller binding pocket of 4D5 mAb (without aromatic side chains) differently affects the vibrational frequencies of Py in comparison to those in *anti*-PAH and 8E11 mAbs.

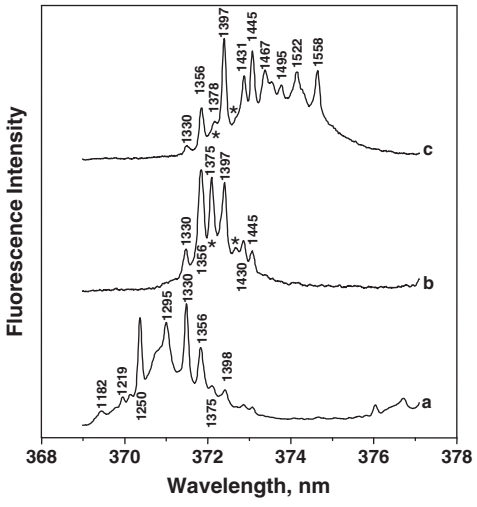

Fig. 5. FLN spectra (4.2 K) of free Py (curve a), Py/4D5 mAb complex (curve b), and Py/*anti*-PAH mAb complex (curve c) in G/PBS glass obtained at 4.2 K. λex = 354 nm; gate width, 200 ns; delay time, 40 ns. A different distribution of several vibrational modes is labeled by stars.

4. Discussion

4.1. Comments on control experiments – specificity of binding

We hasten to add our control experiments (data not shown for simplicity; see also ref. [10]) with bovine IgG, and 2E9 mAb to 4-hydroxyestrone (4-OHE_1)-derived N-acetylcysteine conjugates [29] did not reveal any spectral changes upon incubation with Py. That is, Py did not form any complex with these proteins. This clearly indicates that the different red shifts observed for Py in this work, as shown in Fig. 2 and Table 1, arise from specific interactions of Py with unique binding pockets of 4D5, *anti*-PAH, and 8E11 mAbs. A negligibly small non-specific binding of Py molecule was only observed in the case of 8E11 mAb. However, selective excitation of 364.0 nm used to generate FLN spectra shown in the inset of Fig. 3 (for the Py/8E11 mAb) did not reveal this contribution. However, our NLN and FLN spectra did not reveal any non-specific binding of Py to the 4D5 and *anti*-PAH mAbs that are the focus of this work. This also proves that bovine IgG, 2E9 mAb, and hydrophobic protein sites do not bind Py molecules. The latter indicates the aromatic character of the protein binding pocket is not a sufficient prerequisite for binding PAHs. Apparently, the protein-binding site has to complement the ligand with respect to other means of recognition and strong affinity binding (e.g. steric complementarity, sequence specificity, and possibly a suitable conformational diversity).

4.2. On the origin of conformations I and II

The presence of two different Py populations in *anti*-PAH mAbs and only one population in 4D5 and 8E11 mAbs raises a very important question, namely, what is the origin of the these two (0,0)-bands? Based on the above observations, we suggest the underlying mechanism that distinguishes these populations is the mode of binding. We propose that *anti*-PAH and 8E11 mAbs use π–π interactions (i.e. the binding to aromatic side chains from antibodies) and a π–cation interaction, whereas 4D5 mAb uses only π–cation interaction. The latter is consistent with the absence of aromatic side chains near the planar face of Py in 4D5 mAb. However, all three mAbs must contain Arg and/or Lys that allow the unique locking of Py in conformation I. It cannot be excluded that in some mAbs, pre-existing

conformations could provide proteins the ability to acquire a new function and structure as recently suggested by Tokuriki and Tawfik [1]. The π–cation interaction must be caused by maintaining the orientation of the aromatic ring (the large π-plane of the Py ring) with respect to Arg and/or Lys present within the mAb binding pocket leading to very small Γ_{inh}.

We hasten to add that very narrow (~75 cm^{-1}) origin bands were also observed for the (+)/(−)-*trans*-*anti*-BPDE-dG adducts complexed with 8E11 mAb [25]. This significant reduction in spectral bandwidth suggested these two adducts are also bound tightly in well-defined conformations within the binding pocket, so that molecular motion is restricted (as indicated by the reduced Γ_{inh}, i.e. a narrower distribution of the transition energies). In contrast, the narrowing effect was much less pronounced (i.e. fwhm of ~115–125 cm^{-1}) for the (+)-*cis*-*anti*- and (−)-*cis*-*anti*-BPDE-dG adducts [25]. Since the latter two adducts, based on molecular modeling, are more bulky [30], in this case, the binding most likely involves π–π interactions. This assignment was supported by observed variations in the frequencies of vibrational modes [23]. Finally, we note that π–cation interaction was also suggested to be important in the mAb B[*a*]P-13 (raised against B[*a*]P-butric acid) [31]. These authors suggested high susceptibility of the ELISA, with regard to inorganic ions, could indicate a more hydrophilic binding pocket, e.g. involving a π–cation interaction.

5. Conclusions

Our results support the findings of Pellequer et al. [12] who, based on original modeling studies, reported the first example of a π–cation interaction in which a bound neutral aromatic ligand (BP) was stabilized by a positively charged Arg side chain located in the deep binding pocket of a 4D5 mAb. Comparative studies of Py binding with *anti*-PAH, 8E11, and 4D5 mAbs suggest the binding mode involves only π–cation interaction when the aromatic side chains are not available for antigen stabilization in antibody binding pockets. That is, in the case of conformation I, mAb must contain protons of Arg (and/or Lys) that are close to Py moiety, stabilizing its relative orientation and modifying Py vibrational frequencies. These data suggest simple spectroscopic measurements can be used to provide more insight into the mAb/ligand geometry and operational mode(s) of binding. Further insight into the mode of binding could be provided by studying mAbs for which crystal structures are available, or via mutagenesis studies where the Lys and Arg side groups are eliminated from the Py binding site.

Acknowledgements

Our thanks are due to Professor Regina M. Santella (Columbia University, New York) for providing 8E11 mAb and 4D5 mAb. We also acknowledge Dr. Nhan Dang and Mike Reppert for their experimental help during the early stage of this project. This research was supported by the Johnson Center for Basic Cancer Research at K-State (Manhattan, KS).

References

[1] N. Tokuriki, D.S. Tawfik, Protein dynamism and evolvability, Science 324 (2009) 203–207.
[2] D.M. Webster, A.H. Henry, A.R. Rees, Antibody–antigen interactions, Curr. Opin. Struct. Biol. 4 (1994) 123–129.
[3] L.C. James, D.S. Tawfik, The specificity of cross-reactivity: promiscuous antibody binding involves specific hydrogen bonds rather than nonspecific hydrophobic stickiness, Protein Sci. 12 (2003) 2183–2193.
[4] J.H. Arevalo, M.J. Taussig, I.A. Wilson, Molecular-basis of cross-reactivity and the limits of antibody–antigen complementarity, Nature 365 (1993) 859–863.
[5] S.W.W. Chen, M.H.V. Van Regenmortel, J.L. Pellequer, Structure–activity relationships in peptide–antibody complexes: implications for epitope prediction and development of synthetic peptide vaccines, Curr. Med. Chem. 16 (2009) 953–964.
[6] L.C. James, P. Roversi, D.S. Tawfik, Antibody multispecificity mediated by conformational diversity, Science 299 (2003) 1362–1367.
[7] J. Foote, C. Milstein, Conformational isomerism and the diversity of antibodies, Proc. Natl Acad. Sci. USA 91 (1994) 10370–10374.
[8] J.L. Pellequer, S.W.W. Chen, Y.S. Keum, A.E. Karu, Q.X. Li, V.A. Roberts, Structural basis for preferential binding of non-ortho-substituted polychlorinated biphenyls by the monoclonal antibody S2B1, J. Mol. Recognit. 18 (2005) 282–294.
[9] R. Jankowiak, E.G. Rogan, E.L. Cavalieri, Role of fluorescence line-narrowing spectroscopy and related luminescence-based techniques in the elucidation of mechanisms of tumor initiation by polycyclic aromatic hydrocarbons and estrogens, J. Phys. Chem. B 108 (2004) 10266–10283.
[10] N.M. Grubor, J. Hayes, G.J. Small, R. Jankowiak, Cross-reactivity and conformational multiplicity of an anti-polycyclic aromatic hydrocarbon mAb, Proc. Natl Acad. Sci. USA 102 (2005) 7453–7458.
[11] N.M. Grubor, Y. Liu, X.X. Han, D.W. Armstrong, R. Jankowiak, High resolution spectral differentiation of enantiomers: benzo[a]pyrene tetrols complexed with a promiscuous antibody, J. Am. Chem. Soc. 128 (2006) 6409–6413.
[12] J.L. Pellequer, B.T. Zhao, H.I. Kao, C.W. Bell, K. Li, Q.X. Li, A.E. Karu, V.A. Roberts, Stabilization of bound polycyclic aromatic hydrocarbons by a π–cation interaction, J. Mol. Biol. 302 (2000) 691–699.
[13] D.A. Dougherty, D.A. Stauffer, Acetyl choline binding by a synthetic receptor: implications for biological recognition, Science 250 (1990) 1558–1560.
[14] J.C. Ma, D.A. Dougherty, The cation–π interaction, Chem. Rev. 97 (1997) 1303–1324.
[15] S. Adak, A. Mazumder, R.K. Banerjee, Probing the active site residues in aromatic donor oxidation in horseradish peroxidase: involvement of an arginine and a tyrosine residue in aromatic donor binding, Biochem. J. 314 (1996) 985–991.
[16] R. Jankowiak, Fundamental aspects of fluorescence line-narrowing spectroscopy, in: C. Gooijer, F. Ariese, J.W. Hofstraat (Eds.), Shpol'skii Spectroscopy and Other Site-Selection Methods, John Wiley and Sons, New York, 2000, pp. 235–271.
[17] F. Ariese, R. Jankowiak, High-resolution fluorescence analysis of polycyclic aromatic hydrocarbon derived adducts to DNA and protein, in: C. Gooijer, F. Ariese, J.W. Hofstraat (Eds.), Shpol'skii Spectroscopy and Other Site-Selection Methods, John Wiley and Sons, New York, 2000, pp. 333–362.
[18] A.N. Bader, N.M. Grubor, F. Ariese, C. Gooijer, R. Jankowiak, G.J. Small, Probing the interaction of benzo[a]pyrene adducts and metabolites with monoclonal antibodies using fluorescence line-narrowing spectroscopy, Anal. Chem. 76 (2004) 761–766.
[19] M. Gomes, R.M. Santella, Immunologic methods for the detection of benzo[*a*]pyrene metabolites in urine, Chem. Res. Toxicol. 3 (1990) 307–310.
[20] R.M. Santella, C.D. Lin, W.L. Cleveland, I.B. Weinstein, Monoclonal antibodies to DNA modified by a benzo[*a*]pyrene diol epoxide, Carcinogenesis 5 (1984) 373–377.
[21] A. Nakajima, Solvent effect on vibrational structures of fluorescence and absorption-spectra of pyrene, Bull. Chem. Soc. Jpn 44 (1971) 3272–3277.
[22] K. Kalyanasundaram, J.K. Thomas, Environmental effects on vibronic band intensities in pyrene monomer fluorescence and their application in studies of micellar systems, J. Am. Chem. Soc. 99 (1977) 2039–2044.
[23] V. Glushko, M.S.R. Thaler, C.D. Karp, Pyrene fluorescence fine-structure as a polarity probe of hydrophobic regions—behavior in model solvents, Arch. Biochem. Biophys. 210 (1981) 33–42.
[24] R. Jankowiak, K.P. Roberts, G.J. Small, Fluorescence line-narrowing detection in chromatography and electrophoresis, Electrophoresis 21 (2000) 1251–1266.
[25] B. Miksa, R. Chinnappan, N.C. Dang, M. Reppert, B. Matter, N. Tretyakova, N.M. Grubor, R. Jankowiak, Spectral differentiation and immunoaffinity capillary electrophoresis separation of enantiomeric benzo[a]pyrene diol epoxide-derived DNA adducts, Chem. Res. Toxicol. 20 (2007) 1192–1199.
[26] S.W.W. Chen, J.L. Pellequer, Identification of functionally important residues in proteins using comparative models, Curr. Med. Chem. 11 (2004) 595–605.
[27] M. Suh, F. Ariese, G.J. Small, R. Jankowiak, T.M. Liu, N.E. Geacintov, Conformational studies of the (+)-*trans*-adducts, (−)-*trans*-adducts, (+)-*cis*-adducts, and (−)-*cis*-adducts of *anti*-benzo[a]pyrene diolepoxide to N^2-dG in duplex oligonucleotides using polyacrylamide-gel electrophoresis and low-temperature fluorescence spectroscopy, Biophys. Chem. 56 (1995) 281–296.
[28] Y. Wang, J. Szczepanski, M. Vala, Vibrational spectroscopy of neutral complexes of Fe and polycyclic aromatic hydrocarbons, Chem. Phys. 342 (2007) 107–118.
[29] Y. Markushin, P. Kapke, M. Saeed, H. Zhang, A. Dawoud, E.G. Rogan, E.L. Cavalieri, R. Jankowiak, Development of monoclonal antibodies to 4-hydroxyestrogen-2-N-acetylcysteine conjugates: immunoaffinity and spectroscopic studies, Chem. Res. Toxicol. 18 (2005) 1520–1527.
[30] X.M. Xie, N.E. Geacintov, S. Broyde, Stereochemical origin of opposite orientations in DNA adducts derived from enantiomeric *anti*-benzo[*a*]pyrene diol epoxides with different tumorigenic potentials, Biochemistry 38 (1999) 2956–2968.
[31] T. Scharnweber, M. Fisher, M. Suchanek, D. Knopp, R. Niessner, Monoclonal antibody to polycyclic aromatic hydrocarbons based on a new benzo[a]pyrene immunogen, Fresnius J. Anal. Chem. 371 (2001) 578–585.
[32] W. Humphrey, A. Dalke, K. Schulten, VMD: visual molecular dynamics, J. Mol. Graph. 14 (1996) 33–38.